

4.1 Introduction

The process of glass formation includes the super-cooling of an alloy melt below its glass transition temperature (T_g). As discussed earlier in chapter 1, glass transition refers to the slowing down of the kinetics of liquid dynamics due to super-cooling of melt. The super-cooling plays an important role in formation of glass by increasing the viscosity of metallic melt thereby arresting the constituents of the alloy in a random structure that is away from equilibrium. Kinetically strong glass formers do not show any significant variation in the viscosity at T_g , whereas the glasses which exhibit Arrhenius dependence on temperature (vary significantly with temperature) at T_g are fragile glasses [1-2]. Fragility here does not indicate mechanical behavior, instead it means the reduction in viscosity of the melt with an increase in temperature. All pure metals, water and most of the metallic alloys are kinetically very fragile at their melting point. A most common expression of the relationship between the viscosity and temperature is given by Vogel-Fulcher-Tammann (VFT) equation [3-5]. Doolittle [6] also proposed an expression for variation of viscosity with temperature. Further, many studies have been carried out for studying the free volume of bulk metallic glasses (BMGs) by either direct density measurements [7-10] or by viscosity studies [11-15]. Another model was proposed by Van den Beukel and Sietsma [16] for computing free volume in terms of enthalpy measured by differential scanning calorimetry (DSC). Following this method, many researchers have calculated free volume in terms of enthalpy at temperatures below T_g [8, 10, 17-23].

It is the cooling rate that decides the glass transition process. Higher cooling rate ensures the glass formability at lower temperature, far from the crystallization temperature (T_x). A large gap between T_g and T_x value indicates that the glassy phase is quite far from the crystalline phase and therefore the glassy phase is thermally stable with respect to the crystalline phase. This difference between the crystallization temperature and the glass transition temperature refers to the super-cooled liquid region, i.e., $\Delta T_x = T_x - T_g$. BMGs have very high ΔT_x values ($\approx 10^2$ K) and require very low cooling rates for their synthesis. Formation at low cooling rates enable them to be constructed into different shapes and sizes, such as cylinder, sheet, wires, etc. This escalates their position as structural material to the foremost level. Their thermodynamics and physical properties strongly depend upon their cooling process. In fact, cooling rate is the prime factor that influences the glass forming ability (GFA) of metallic glasses. With an increase in cooling rate, the time required for the constituents to acquire a stable configuration decreases and the viscosity of the melt increases. Due to this the molecules do not get sufficient time to reach equilibrium and they get trapped in a liquid-like structure. This propels the system away from equilibrium with a very low free volume available at T_g . Hence, high cooling rates facilitate the process of glass formation. In order to attain a glassy alloy, the formation of smallest observable crystalline structure (i.e., the volume fraction $\approx 10^{-6}$) must be suppressed. The equation that correlates the cooling rate and the crystallized volume fraction during solidification process is as follows [4.24-4.25]:

$$X(T) = \frac{4\pi}{3R^4} \int_{T_i}^{T_g} I(T') \left[\int_{T''}^{T_g} u(T'') dT'' \right]^3 dT' \quad (4.1)$$

Where I and u are the steady state nucleation and growth rates, T_g and T_l are the glass transition and the liquidus temperatures respectively, $X(T)$ is the crystallized fraction and R is the cooling rate. When $X(T)$ is taken as 10^{-6} , then R becomes R_c , i.e., the critical cooling rate. The critical cooling rate (R_c) can be understood as the minimum cooling rate required for the formation of a fully amorphous alloy. Equation 4.1 can be used to evaluate R_c in terms of I and u , as given below:

$$R_c^4 = \frac{4\pi}{3 \times 10^{-6}} \int_{T_l}^{T_g} I(T') \left[\int_{T'}^{T_g} u(T'') dT'' \right]^3 dT' \quad (4.2)$$

Another way to experimentally determine the value of R_c is by constructing time-temperature-transformation diagram (TTT diagram). Fig 4.1 represents a typical TTT diagram with time and temperature on x-axis and y-axis respectively.

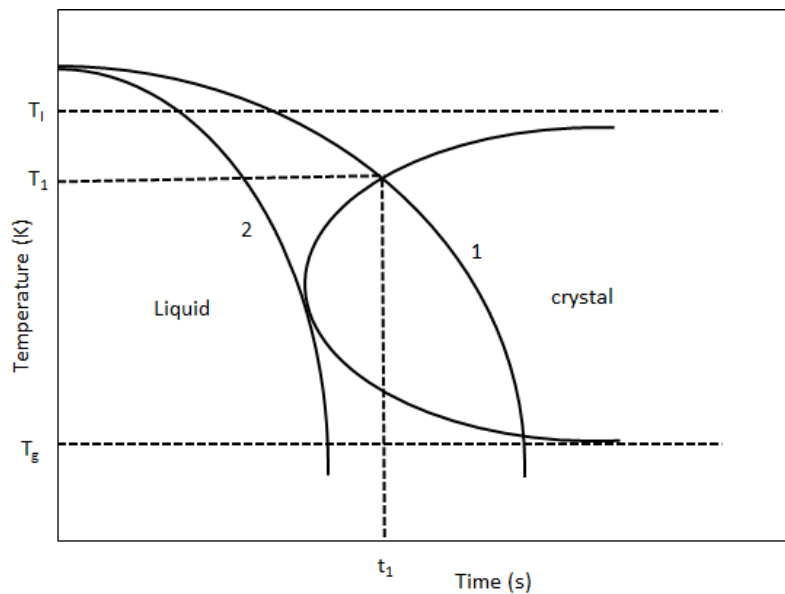


Fig. 4.1: Schematic TTT diagram

It consists of a C-shaped curve which indicates the formation of crystalline phase during solidification of a melt from T_l to T_g . Curve 1 and 2 represents two cooling experiments. When an alloy is cooled at smaller cooling rates as curve 1, its crystallization occurs at (T_l, t_l) . But if cooling is done at higher rates as curve 2, the crystallization is suppressed and a glassy structure is obtained if cooled below T_g . Curve 2 provides the value of R_c . Any metallic melt when cooled at a rate higher than its R_c will transform into a glassy phase below T_g . But if cooling rate is lower than R_c , the resulting solid may not be a homogeneous glassy alloy. In other words, glass formation can only take place if the liquid is cooled at a rate greater than its R_c and below T_g . Hence, R_c is one of the conclusive criterion for glass formation. A smaller value of R_c represents good glass formability of metallic glass.

Basically TTT diagrams express the competition between the driving force of crystallization and the atomic mobility. With decrease in temperature, atomic mobility decreases, but the driving force of crystallization increases. At the nose of the TTT diagram, both the atomic mobility and the driving force of crystallization balance each other. If the time and temperature of the nose of TTT diagram is known, then the value of R_c can be calculated using the below equation:

$$R_c \cong \frac{T_l - T_n}{t_n} \quad (4.3)$$

Where, T_l and T_n are the liquidus and nose temperature, and t_n is the nose time. The limitation of the nose method is that it overestimates the R_c value [4.26]. Further Barandiaran and Colmenero [4.27] proposed a method for the determination of R_c .

$$\ln R = A - \frac{B}{(T_l - T_{xc})^2} \quad (4.4)$$

Where, R is the cooling rate, A & B are constants, T_l is the liquidus temperature and T_{xc} is the onset temperature of crystallization during solidification.

Another experimental parameter for the determination of the glass formability is the critical dimension (Z_{max}). It refers to the maximum attainable size of a fully amorphous alloy. A greater Z_{max} indicates a better ability of an amorphous alloy to form a bulk metallic glass (BMG). Lin and Johnson [4.28] gave a relation to correlate Z_{max} and R_c :

$$R_c = \frac{10}{Z_{max}^2} \quad (4.5)$$

These two parameters (R_c and Z_{max}) are experimental parameters that give the estimate of the glass forming ability of a metallic glass. “*Glass forming ability (GFA)*” is basically the ability of any alloy to form glass by suppressing crystallization. It involves the ability of any metallic melt to avoid crystallization during cooling and the stability of the corresponding liquid phase in undercooled state.

Assuming steady state nucleation, the nucleation rate can be evaluated by the product of thermodynamic and kinetic factor [4.29]:

$$I = AD \exp \left[-\frac{\Delta G^*}{kT} \right] \quad (4.6)$$

Where A is a constant, k is Boltzmann’s constant, T is temperature, D the effective diffusivity and ΔG^* is the activation energy which must be overcome for the formation of stable nuclei.

ΔG^* can be expressed as:

$$\Delta G^* = \frac{16\pi\sigma^3}{3(\Delta G)^2} \quad (4.7)$$

Where, σ is the interfacial energy between the liquid and the crystalline phase and ΔG is the Gibbs free energy difference between the liquid and corresponding crystalline phase. ΔG also known as the driving force of crystallization. Hence, the structural, kinetic and the thermodynamic factor (ΔG) are the crucial factors regarding the glass formation in amorphous alloys.

4.1.1 Thermodynamic Aspect

The prime reason behind the formation of a glass from a metallic melt during its cooling process is the lack of appropriate number of crystal nucleation sites. A large thermodynamic driving force and a rapid kinetics of crystal nucleation aids the process of crystal nucleation. With the initiation of the cooling process, the molecules of metallic glass either tend to move towards their equilibrium state or get super-cooled, depending on the amount of the thermodynamic driving force available and the briskness of crystallization kinetics. The thermodynamic driving force can be calculated in terms of Gibbs free energy difference (ΔG) between the super-cooled liquid and the corresponding crystalline phase. Generally, good glass formers exhibit low driving force, i.e., lower ΔG value, which results in low nucleation rates and hence a better GFA. Also smaller ΔS value indicates a better GFA, as it increases the disorder of the super-cooled liquid state and hence enhances its amorphicity. As supercooling increases, ΔS decreases and reaches a minimum value at T_g , where the material

gets converted into solid phase. It is presumed that if a liquid is cooled below its T_g , there lies a possibility that ΔS vanishes, i.e., the entropy of glassy phase becomes equal to the entropy of the crystalline phase. Hence the glassy phase becomes as stable as the crystalline phase when $\Delta S \rightarrow 0$. The temperature at which this happens is termed as Kauzmann temperature (T_K). However, practically the super-cooling of a melt below its T_g is not possible since the material gets converted into solid well before T_K (i.e., at T_g). Hence, the concept of an amorphous material having equal entropy as that of its crystalline counterpart becomes self-contradictory. This concept is termed as “Kauzmann paradox” since it was brought forward by Walter Kauzmann in 1948 [4.30].

4.2 Theoretical Formulations

4.2.1 Different Expressions of ΔG

The thermodynamic driving force, i.e., Gibbs free energy difference (ΔG) between the super-cooled liquid and the corresponding crystalline phase, can be determined by the following equation:

$$\Delta G = \Delta H - T\Delta S \quad (4.8)$$

$$\text{Where, } \Delta H = \Delta H_m - \int_T^{T_m} \Delta C_p dT \quad (4.9)$$

$$\text{and } \Delta S = \Delta S_m - \int_T^{T_m} \frac{\Delta C_p}{T} dT \quad (4.10)$$

Where, ΔH_m , ΔS_m and T_m are the melting enthalpy, entropy and temperature respectively and they are related by the following expression:

$$\Delta H_m = \Delta S_m T_m \quad (4.11)$$

ΔC_p , defined as $C_p^l - C_p^x$, is the difference in specific heats of liquid and corresponding crystalline phase. If the experimental specific heat data is available for under-cooled liquid and crystal phases, then the experimental ΔG can be calculated using eq. (4.8) - (4.10). But in absence of experimental data we have to switch to approximations i.e., expressing temperature dependence of ΔC_p in a suitable way. Plenty of approximations have been made to derive various expressions of ΔG . In absence of any experimental data of ΔC_p , Turnbull [4.31] assumed $\Delta C_p = 0$ thereby giving the following expression:

$$\Delta G = \frac{\Delta H_m \Delta T}{T_m} \quad (4.12)$$

Hoffman [4.32] assumed two conditions, namely; (1) ΔC_p is a non-zero constant, (2) the difference in enthalpy between the two phases vanishes at a temperature T_∞ , slightly below the glass transition temperature T_g , of the liquid.

For constant ΔC_p , eq. (4.9) can be written as:

$$\Delta H = \Delta H_m - \Delta C_p (T_m - T) \quad (4.13)$$

Since, $\Delta H=0$, at $T=T_\infty$

$$\Delta C_p = \frac{\Delta H_m}{T_m - T_\infty} \quad (4.14)$$

On substituting eqs. (4.13) & (4.14) in eq. (4.9) and (4.10), and using eq. (4.8), we get

$$\Delta G = \frac{\Delta H_m \Delta T}{T_m} \left(\frac{T}{T_m} \right) + \frac{\Delta H_m \Delta T}{T_m} \left(\frac{\Delta T}{T + T_m} \right) \left(\frac{T}{T_m} - \frac{T_\infty}{T_m - T_\infty} \right) \quad (4.15)$$

When ΔT is small, $\frac{\Delta T}{T + T_m}$ is negligible and at $T = T_g$; $\frac{T_\infty}{T_m - T_\infty} \cong \frac{T}{T_m}$. So the last term in eq.

(4.15) becomes zero, leading to the Hoffman's expression.

$$\Delta G = \frac{\Delta H_m \Delta T}{T_m} \left(\frac{T}{T_m} \right) \quad (4.16)$$

Further, considering ΔC_p to be a constant Jones and Chadwick (J & C) [4.33] proposed the following expression:

$$\Delta G = \frac{\Delta H_m \Delta T}{T_m} - (\Delta T^2) \left(\frac{\Delta C_p^m}{T_m + T} \right) \quad (4.17)$$

Following this many other researchers [4.34-4.40] gave expressions based on constant ΔC_p approximation.

Treating ΔC_p to be constant in the undercooled region eq. (4.10) becomes

$$\Delta S = \frac{\Delta H_m}{T_m} - \Delta C_p \ln \left(\frac{T_m}{T} \right) \quad (4.18)$$

Considering $\Delta S = 0$ at Kauzmann temperature (T_K), one can easily get

$$\Delta C_p = \alpha \frac{\Delta H_m}{T_m} \quad (4.19)$$

$$\text{With } \alpha = \frac{1}{\ln T_m / T_K} \quad (4.20)$$

Using these relations and approximating $\ln \frac{T_m}{T} \cong \frac{2\Delta T}{T_m + T}$, Thomson and Spaepen (T-S) [4.34]

have derived a general formula

$$\Delta G = \frac{\Delta H_m \Delta T}{T_m} \left[\frac{(1-\alpha)T_m + (1+\alpha)T}{T_m + T} \right] \quad (4.21)$$

$$\text{When } \alpha \cong 1, \Delta C_p = \frac{\Delta H_m}{T_m} \quad (4.22)$$

Substituting this value in J & C expression (eq. (4.17)), T-S [4.34] arrived at the simple expression

$$\Delta G = \frac{\Delta H_m \Delta T}{T_m} \left(\frac{2T}{T_m + T} \right) \quad (4.23)$$

This equation is only valid for small ΔT , and leads to error in calculations of ΔG values at larger undercooling. Generally, multicomponent metallic glasses exhibit larger undercooling range. Hence, eq. (4.23) cannot be used for a wide range of metallic glasses. Hence, Lad et al [4.35] modified the Eq. (4.23) by considering

$$\ln \frac{T_m}{T} \cong \frac{\Delta T}{T} \left(1 - \frac{\Delta T}{2T} \right) \quad (4.24)$$

Considering ΔC_p to be constant and using eqs. (4.8-4.10) and (4.24), Lad et al deduced an expression as

$$\Delta G = \frac{\Delta H_m \Delta T}{T_m} \left(1 - \frac{\Delta T}{2T} \right) \quad (4.25)$$

Eqs. (4.23) & (4.25) represented large deviation of ΔG values from the experimental data, when applied to multicomponent metallic alloys like $\text{Pd}_{40}\text{Cu}_{30}\text{Ni}_{10}\text{P}_{20}$. So, again Lad et al modified eq. (4.25).

Again considering ΔC_p to be constant and approximating $\ln\left(\frac{T_m}{T}\right) \cong \frac{4T\Delta T}{(T_m + T)^2}$, Lad et al

[4.36] obtained

$$\Delta G = \frac{\Delta H_m \Delta T}{T_m} \left(\frac{4T^2}{(T + T_m)^2} \right) \quad (4.26)$$

This equation has been tested for various multicomponent alloys and found satisfactory results with the experimental data at larger undercooling.

According to Battezzati and Garrone (B & G) [4.37], the expression for ΔG is given as follows:

$$\Delta G = \Delta S_m (T_m - T) - \gamma \Delta S_m \left[(T_m - T) - T \ln(T_m / T) \right] \quad (4.27)$$

Where, γ parameter in above equation is represented as:

$$\gamma = \frac{(1 - \Delta H_x / \Delta H_m)}{(1 - T_x / T_m)} \quad (4.28)$$

Where the terms have their usual meanings

On substituting the value of ΔC_p from eq. (4.19) in eq. (4.9) and eq. (4.10) and using the so obtained values of ΔH and ΔS in eq. (4.8), Dhurandhar et al [4.38] derived the following expression of ΔG :

$$\Delta G = \frac{\Delta H_m}{T_m} \left[\alpha T \ln \frac{T_m}{T} + \Delta T(1 - \alpha) \right] \quad (4.29)$$

The value of α can be evaluated by taking the constant value of $\Delta C_p = \Delta C_p^m$ at melting point in eq. (4.29) as

$$\alpha = \frac{\Delta C_p^m T_m}{\Delta H_m} \quad (4.30)$$

However, in most of the glass forming systems the specific heat difference increases with undercooling, so for such kind of systems ΔC_p at any temperature in the undercooled region can be assumed to be either linearly or hyperbolically dependent on T .

Singh and Holz (S & H) [4.39] gave the following expression for linear variation of ΔC_p with T :

$$\Delta G = \frac{\Delta H_m \Delta T}{T_m} \left(\frac{7T}{T_m + 6T} \right) \quad (4.31)$$

Ji & Pan [4.40] considered hyperbolic variation of ΔC_p with T ($\Delta C_p = \Delta H_m / T$) and derived the following expression:

$$\Delta G = \frac{2\Delta H_m \Delta T}{T_m} \left(\frac{T}{T_m + T} - \frac{\Delta T^2 T_m}{3(T_m + T)^3} \right) \quad (4.32)$$

Further, Dhurandhar et al [4.38] gave another expression of ΔG dependent on hyperbolic variation of ΔC_p i.e., $\Delta C_p = \frac{\Delta C_p^m T_m}{T}$

Substituting ΔC_p in equations (4.9) & (4.10) and using eq. (4.8), the ΔG expression can be represented by the following equation:

$$\Delta G = \frac{\Delta H_m \Delta T}{T_m} - \Delta C_p^m T_m \left[\ln \frac{T_m}{T} - \frac{\Delta T}{T_m} \right] \quad (4.33)$$

Another expression for hyperbolic variation of ΔC_p with T is given by:

$$\Delta C_p = \frac{C}{T} + D \quad (4.34)$$

On substituting ΔC_p from the above equation in Eq. (4.9) and (4.10) and simplifying Eq. (4.8), Patel et al derived [4.41] the following expression

$$\Delta G = \frac{\Delta H_m \Delta T}{T_m} + \ln \frac{T_m}{T} (DT - C) - \Delta T \left(D - \frac{C}{T_m} \right) \quad (4.35)$$

The unknown constants A and B can be easily calculated in terms of known experimental parameters, by utilizing the condition that ΔS becomes zero at Kauzmann temperature, T_K :

$$C = \frac{\Delta H_m - T_m \Delta C_p^m \ln \frac{T_m}{T_K}}{\frac{T_m - T_K}{T_K} - \ln \frac{T_m}{T_K}} \quad (4.36)$$

And

$$D = \Delta C_p^m - \frac{C}{T_m} \quad (4.37)$$

According to the available experimental details of ΔC_p , any of these expressions can be used for the calculations of ΔG . Further, single expression is not sufficient to express the temperature dependence of ΔG for all BMGs, since different BMGs show different temperature dependence of ΔC_p . In present chapter, the thermodynamic parameter ΔG , as a function of temperature, is calculated for $\text{Au}_{49}\text{Ag}_{5.5}\text{Pd}_{2.3}\text{Cu}_{26.9}\text{Si}_{16.3}$ metallic glass using

various expressions available and the results are compared with the respective experimental values of ΔG in order to find the best theoretical expression of ΔG . Further, the thermodynamic behavior of $\text{Au}_{49}\text{Ag}_{5.5}\text{Pd}_{2.3}\text{Cu}_{26.9}\text{Si}_{16.3}$ metallic glass is also studied based on the thermodynamic parameters ΔH and ΔS . The detailed formulation and the results for thermodynamic properties along with the comparison with the experimental results are given in this chapter of thesis.

4.2.2 GFA Parameters

The information about the GFA has an important place in study of BMGs as it gives a clear indication about mechanism of glass formation, which thereby provides a better design of new BMG. Inoue [4.42] gave a set of empirical rules for glass formation that are as follows:

- (i) “Three or more than three components” enhance the process of glass formation.
- (ii) “Size mismatch between the components” also favor glass formation. The atomic sizes of different constituents must differ by 12% for achieving a good GFA.
- (iii) “Negative heat of mixing” should be there among the constituents of the glass forming alloy.

The empirical rules given by Inoue et al. [4.42] and Johnson [4.43] have significantly contributed to the understanding of GFA of BMGs, with some exceptions [4.44].

The GFA of BMGs may be accessed in terms of some quantitative parameters, that make use of the liquidus, melting, crystallization and glass transition temperatures (T_l , T_m , T_x and T_g respectively). Some of these theoretical GFA parameters are reported in table 4.1. In some

cases, these GFA parameters may provide correct information about the GFA of metallic glasses. But their accountability cannot be extended to whole class of metallic glasses. Identification of the best GFA parameter is vital for finding the best glass former. Therefore in order to find the best GFA parameter, the GFA parameters are correlated with R_c (or Z_{max}).

Table 4.1 Various GFA parameters

GFA Parameters	Formula	Reference
ΔT_x	$T_x - T_g$	[4.45]
T_{rg}	T_g/T_l	[4.46]
γ	$T_x/(T_g + T_l)$	[4.47]
β'	$T_x T_g / (T_l - T_x)^2$	[4.48]
δ	$T_x / (T_l - T_g)$	[4.49]
γ_m	$(2T_x - T_g) / T_l$	[4.50]
α	T_x / T_l	[4.51]
β	$T_x / T_g - T_g / T_l$	[4.51]
ζ	$T_g / T_l - \Delta T_x / T_x$	[4.52]
ω'	$(T_g / T_x) - (2T_g / (T_g + T_l))$	[4.53]
ω_2	$T_g / (2T_x - T_g) - (T_g / T_l)$	[4.54]
ϕ	$T_{rg} (\Delta T_x / T_g)^{0.143}$	[4.55]
γ_c	$(3T_x - 2T_g) / T_l$	[4.56]
ω	$T_l(T_l + T_x) / T_x(T_l - T_x)$	[4.57]
ΔT_{rg}	$(T_x - T_g) / (T_l - T_g)$	[4.58]

Here, T_g , T_x , and T_l are the glass transition temperature, crystallization temperature and liquidus temperature respectively and ΔH_m and ΔH_x are the enthalpy of melting and crystallization respectively.

The applicability of these GFA parameters have been checked by analyzing their relationship with Z_{max} for Zr-based metallic glasses. Apart from the GFA parameters, the thermodynamic parameter $\Delta G(T_g)$ is also evaluated and its relationship with Z_{max} is studied for Zr-based metallic glasses. Moreover, effect of minor substitution of alloying elements such as Al, Nb, Co, etc. on the GFA of Cu-Zr and Fe-based metallic glasses have also been studied.

4.3 Results and Discussions

The metastable character of an amorphous alloy makes it a suitable candidate for studying its sensitivity towards thermal treatment. On application of heat, the glassy structure moves toward stable crystalline configuration. A poor glass former crystallizes more easily as compared to a good glass former. The GFA of a metallic glass can be studied by thermodynamic parameters, i.e., the Gibbs free energy difference (ΔG), the enthalpy difference (ΔH), and the entropy difference (ΔS), between the undercooled liquid phase and the corresponding crystalline phase. A better glass former is known for its low driving force of crystallization, i.e., smaller value of ΔG . Also, a smaller ΔS indicates greater stability of liquid phase against crystalline phase, and hence a better GFA.

4.3.1 Thermodynamic Study of $\text{Au}_{49}\text{Ag}_{5.5}\text{Pd}_{2.3}\text{Cu}_{26.9}\text{Si}_{16.3}$ Metallic Glass

Au-based amorphous alloys are known for their mechanical strength and corrosion resistance, due to which they find potential applications in various scientific and engineering disciplines. Initially the maximum achievable thickness of binary $\text{Au}_{75}\text{Si}_{25}$ metallic glass, by developed by Duwez and coworkers [4.59], was below $50\mu\text{m}$. subsequently, the GFA of binary Au-Si metallic glass was enhanced by partially substituting Au and Si by different elements. It was found that partial substitution of Si by Ge enhances the GFA of Au-Si metallic glass [4.60]. Another Au-based metallic glass, having composition $\text{Au}_{49}\text{Ag}_{5.5}\text{Pd}_{2.3}\text{Cu}_{26.9}\text{Si}_{16.3}$, with a critical diameter of 5mm was reported by Schroers et al [4.61]. This metallic glass is potential material for applications in the fields of medical, dental and micro-electro-mechanical systems (MEMS), due to its superior qualities such as high hardness, toughness, and oxidation and corrosion resistance. Tang et al [4.62] have studied the thermo-mechanical properties of Au–Ag–Pd–Cu–Si bulk metallic glass. Recently, Mechler et al [4.63] studied the phenomena of surface freezing in $\text{Au}_{49}\text{Ag}_{5.5}\text{Pd}_{2.3}\text{Cu}_{26.9}\text{Si}_{16.3}$ metallic glass. They suggested that the bulk metallic glass forming alloy $\text{Au}_{49}\text{Ag}_{5.5}\text{Pd}_{2.3}\text{Cu}_{26.9}\text{Si}_{16.3}$ consists of a two-dimensional crystalline monolayer phase at temperatures about 50 K above the eutectic temperature.

The thermodynamics of $\text{Au}_{49}\text{Ag}_{5.5}\text{Pd}_{2.3}\text{Cu}_{26.9}\text{Si}_{16}$ metallic glass has been studied by calculating the thermodynamic parameters ΔG , ΔS and ΔH . ΔG values has been calculated in the entire undercooled region by different expressions available in literature, and the

results are compared with experimental ΔG . Turnbull derived an expression for ΔG considering ΔC_p to be zero, but it provides very crude results for metallic glasses. Many other expressions have been developed by considering ΔC_p to be constant. These expressions may provide good results for few metallic glasses. However, in most metallic glasses the specific heat difference varies appreciably with temperature and for such cases the constant ΔC_p assumption shows large deviations in the ΔG values. Hence, the information about the variation of ΔC_p with temperature is necessary for computing ΔG accurately. Another important point to note is that all the expressions given by previous workers consider relatively small undercooled region ($\Delta T = T_m - T$) and hence approximate the $\ln(T_m/T)$ term using Taylor series expansion either up to first or second order. This limits the applicability of their expressions to small undercooled region and hence shows deviation of theoretically calculated values from experimental points in the large undercooled region. Hence one must switch to other expressions based on temperature dependent expressions of ΔC_p . Mostly, all glass forming systems show an increase in ΔC_p with increasing undercooling (ΔT). According to a previous study on the thermodynamics of the $\text{Au}_{49}\text{Ag}_{5.5}\text{Pd}_{2.3}\text{Cu}_{26.9}\text{Si}_{16.3}$ glass-forming alloy [4.64], it was found that ΔC_p decreases hyperbolically with increasing temperature. Hence, assuming ΔC_p to be constant throughout may provide crude result for $\text{Au}_{49}\text{Ag}_{5.5}\text{Pd}_{2.3}\text{Cu}_{26.9}\text{Si}_{16.3}$ amorphous alloy.

Fig. 4.2 represents the variation of ΔG with temperature in the entire undercooled region. Few expressions provide results very close to experimental data, such as those calculated by expressions given by T-S, Ji & Pan, B & G, Dhurandhar et al and Patel et al. T-S and Ji &

Pan expressions are based on constant ΔC_p approximation and involves respectively first and third order Taylor series expansion of $\ln(T_m/T)$ term. B & G expression contains a constant γ (eq. 4.28) that is supposed to be equal to 0.8 for all metallic glasses [B&G]. But, this parameter γ may take different values depending on the crystallization and melting enthalpy, and their corresponding characteristic temperatures, according to eq. (4.28). Moreover, for a system undergoing crystallization in multiple steps, it becomes difficult to choose correct step for the calculation of γ . Also, the enthalpies and temperatures involved in the calculation of γ are heating rate dependent. Hence it cannot be considered to be a constant. Therefore, B & G expression must take the variable nature of γ parameter into account before applying it to glassy alloys. γ is found to be 1.19 for $\text{Au}_{49}\text{Ag}_{5.5}\text{Pd}_{2.3}\text{Cu}_{26.9}\text{Si}_{16.3}$ metallic glass.

The expressions given by Dhurandhar et al (eq. (4.33)) and Patel et al (eq. (4.35)), considering hyperbolic variation of ΔC_p with temperature, are more appropriate for the calculations of ΔG , ΔH and ΔS for this particular amorphous alloy. The expressions given by Patel et al require the knowledge of Kauzmann temperature (T_K), which is found by extrapolating ΔS curve to zero. Here we have taken the experimental value of T_K given by Fontana et al [4.64]. Figures 4.3 and 4.4 represent the variation of ΔH and ΔS respectively with temperature, as calculated by expressions given by Patel et al [4.41] by considering hyperbolic variation of ΔC_p with temperature. Both ΔH and ΔS curves superimpose their respective experimental curves, showing the validity of expressions given by Patel et al [4.41] in the entire undercooled region.

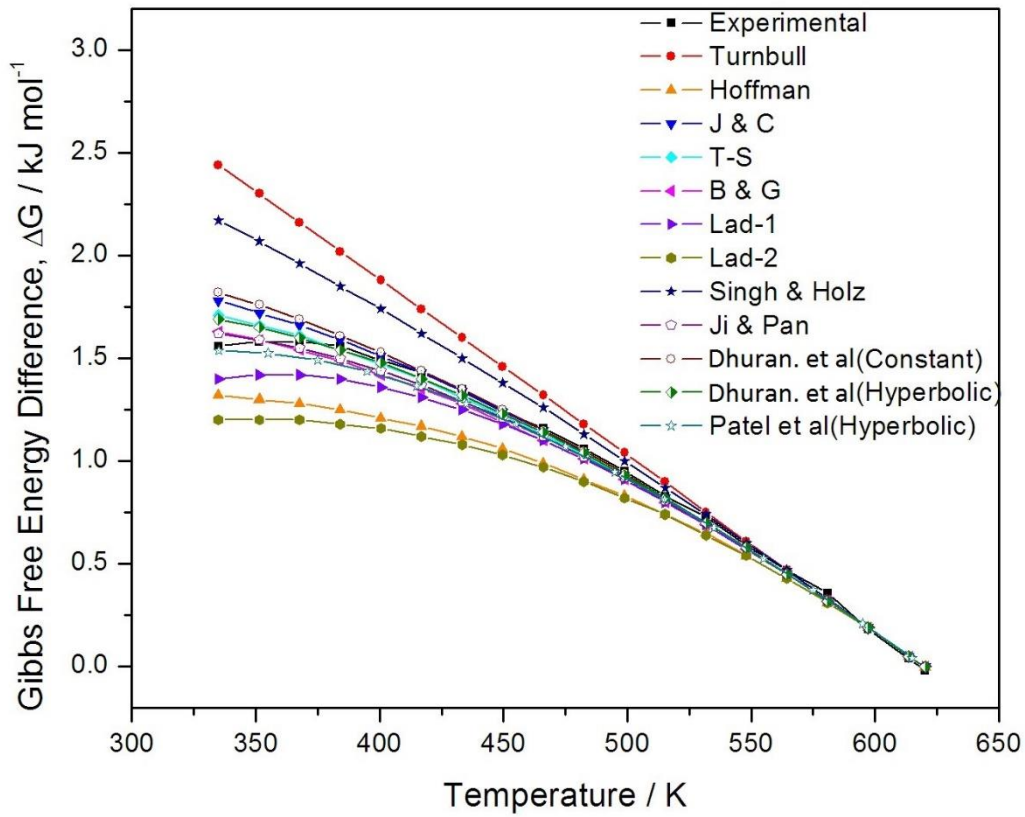


Fig. 4.2: Variation of ΔG with temperature for $\text{Au}_{49}\text{Ag}_{5.5}\text{Pd}_{2.3}\text{Cu}_{26.9}\text{Si}_{16.3}$ metallic glass

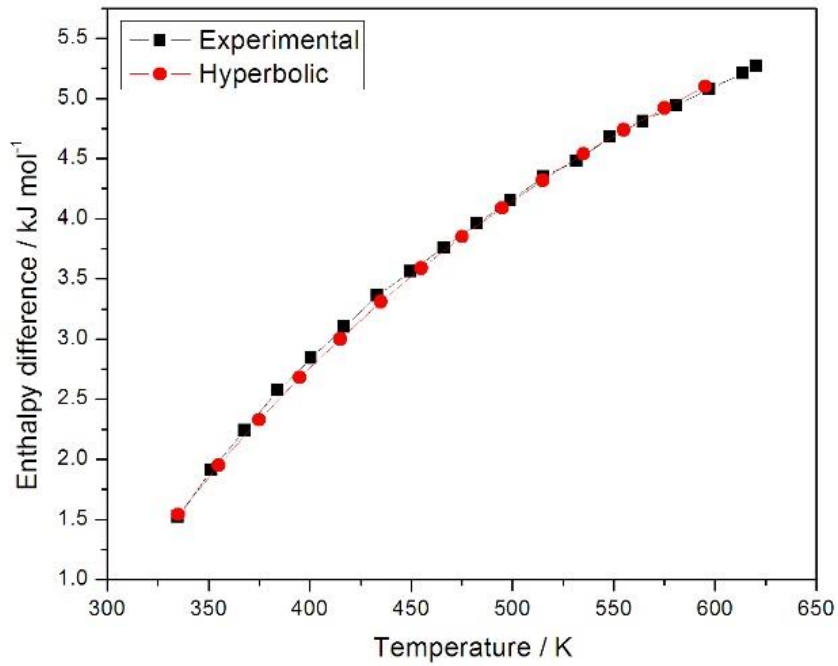


Fig. 4.3: Variation of ΔH with temperature for $\text{Au}_{49}\text{Ag}_{5.5}\text{Pd}_{2.3}\text{Cu}_{26.9}\text{Si}_{16.3}$ metallic glass

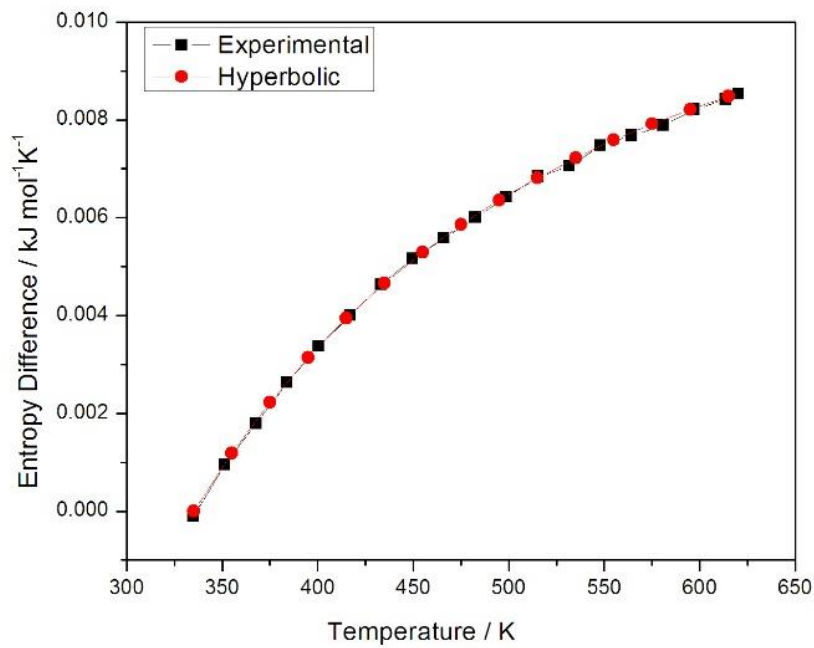


Fig. 4.4: Variation of ΔS with temperature for $\text{Au}_{49}\text{Ag}_{5.5}\text{Pd}_{2.3}\text{Cu}_{26.9}\text{Si}_{16.3}$ metallic glass

4.3.2 Relationship Between GFA Parameters and Critical Dimension for Zr-based Metallic Glasses

The ability of a liquid to resist crystallization during cooling process, and hence to get supercooled into a state of rigidity, is considered as the glass forming ability. Further, the thermal stability of the liquid phase upon cooling assists the progress of the formation of glassy state. The information about the glass forming ability of metallic glasses can be procured by knowledge of the experimental parameter R_c i.e., the critical cooling rate. R_c can be understood in terms of the minimum cooling rate sufficient enough to avoid the formation of any undesired phase, which in case of metallic glasses is the crystalline phase. A greater value of R_c implies that the system requires a high cooling rate for suppressing the crystallization event, and hence lower is the GFA. Experimentally, R_c is considered to be the best GFA criteria. Another experimental parameter is critical dimension, Z_{max} . Z_{max} is the maximum attainable size of fully amorphous material, which decreases with an increase in R_c [4.65]. This implies that a good glass former will have a larger value of Z_{max} as compared to a poor glass former. But determination of R_c (or Z_{max}) involves a series of continuous cooling experiments, which itself is a tedious job. So, in order to make the work easier a variety of GFA parameters have been formulated by researchers [4.46-4.58], depending on the characteristic temperatures, such as the glass transition temperature (T_g), the crystallization temperature (T_x), the melting and liquidus temperature (T_m and T_l respectively). In order to check the validity of these GFA parameters, they have been correlated with Z_{max} for five Zr-based Metallic glasses ($Zr_{65}Al_{8.7}Cu_{14.4}Ni_{11.9}$,

Zr₆₄Al_{10.1}Cu_{11.7}Ni_{14.2}, Zr_{63.5}Al_{10.7}Cu_{10.7}Ni_{15.1}, Zr₆₃Al_{11.4}Cu_{9.3}Ni_{16.3}, and Zr_{62.5}Al_{12.1}Cu_{7.95}Ni_{17.45}). Table 4.2 reports the values of the experimental parameters (T_g , T_x , T_m , ΔH_m and Z_{max} as taken from reference [4.66]).

Table 4.2 Experimental parameters for Zr-based metallic glasses [4.66]

Alloy Compositions	ΔH_m (kJmol ⁻¹)	Z_{max} (mm)	T_g (K)	T_x (K)	T_m (K)
Zr _{62.5} Al _{12.1} Cu _{7.95} Ni _{17.45}	19.39	7.5	668±1	738±1	1111±1
Zr ₆₃ Al _{11.4} Cu _{9.3} Ni _{16.3}	19.52	6.5	663±1	732±1	1103±1
Zr _{63.5} Al _{10.7} Cu _{10.7} Ni _{15.1}	19.65	6	653±1	724±1	1100±1
Zr ₆₄ Al _{10.1} Cu _{11.7} Ni _{14.2}	19.76	5	657±1	717±1	1098±1
Zr ₆₅ Al _{8.7} Cu _{14.4} Ni _{11.9}	20.02	4	647±1	709±1	1125±1

The GFA of these Zr-based metallic glasses have been analyzed using the GFA parameters mentioned in table 4.1. All the aforementioned parameters were correlated with Z_{max} , for identifying the best GFA parameter. Figures 4.5 (a) to 4.5 (f) represents the variation of various GFA parameters with Z_{max} . Among various available GFA parameters, the reduced glass transition temperature (T_{rg}) [4.46] and the super-cooled liquid region (ΔT_x) [4.45] are the most widely used ones. T_{rg} is defined as the ratio of glass transition temperature (T_g) and liquidus temperature (T_l). good glass formers tend to have T_{rg} values in the range 0.66-0.69. Here, in the case of Zr-based metallic glasses T_{rg} varies from 0.55-0.57. Zr_{63.5}Al_{10.7}Cu_{10.7}Ni_{15.1} metallic glass with $T_{rg} = 0.565$ is a better glass former than Zr₆₄Al_{10.1}Cu_{11.7}Ni_{14.2} with $T_{rg} 0.568$. Hence, T_{rg} does not provide correct information about the variation of GFA in Zr- based metallic glasses. ΔT_x can be understood as the difference

between the T_x and T_g . Large difference between T_x and T_g indicates that the material takes more time to crystallize, thereby showing better stability against crystallization. ΔT_x indicates the stability of supercooled liquid against crystallization. Generally, glass formers are supposed to have values of ΔT_x to be in the range 16.3-117. Cai et al [4.66] have shown that these two parameters (T_{rg} and ΔT_x) cannot be used for studying the GFA of Zr-based metallic glasses, since they do not vary linearly with Z_{max} . Another GFA indicator γ proposed by Lu and Liu [4.47] is one of the good indicators of GFA with values ranging between 0.35-0.50 for good glass formers. In present case, $Zr_{62.5}Al_{12.1}Cu_{7.95}Ni_{17.45}$ is found to be the best glass former ($\gamma = 0.40$) among all the five compositions. Furthermore, the parameters β' [4.48] and δ [4.49] were proposed depending on the classical nucleation and growth theory. Both of these parameters show a linear variation with Z_{max} as observed from figure 4.5 (a). Several other GFA indicating criterion, such as γ_m [4.50], α [4.51], β [4.51], ζ [4.52], and ω' [4.53], ω_2 [4.54], based on the stability of liquid phase against competing crystalline phase and the resistance of amorphous phase against crystallization, have been formulated by various researchers in the past. The parameter α is supposed to be applicable for studying the GFA of metallic glasses where a distinct T_g is not observed [4.51]. The relationship of γ_m , α , β , ζ , ω' , and ω_2 with Z_{max} is shown in figures 4.5 (a-c). Extending the applicability of GFA criteria from metallic glasses to network and molecular glasses, Fan et al [4.55] proposed a criterion namely φ based on the concepts of nucleation theory and fragility. Depending upon the relation between cooling and heating process, Guo and Liu [4.56] formulated another GFA parameter γ_c . Fig 4.5 (d) represents the relation of φ and γ_c with Z_{max} . Based on

the Gibbs free energy difference between the supercooled liquid phase and the corresponding crystalline phase, Ji and Pan [4.57] formulated thermodynamic parameter ω , for evaluation of GFA of metallic glasses and oxide glasses. This parameter ω also shows a positive correlation with Z_{max} (Fig. 4.5 (e)). The variation of the reduced supercooled region (ΔT_{rg}) [4.58] with Z_{max} is shown in fig 4.5 (f). R^2 value for ΔT_{rg} - Z_{max} plot is 0.67, which indicates that ΔT_{rg} is not an appropriate parameter for studying GFA of Zr-based metallic glasses. All the GFA parameters show good correlation with Z_{max} for Zr-based metallic glasses, with values of R^2 ranging from 0.8 to 0.95, except for T_{rg} , ΔT_x , and ΔT_{rg} . The thermodynamic parameter ΔG at T_g is calculated by using equations (4.25) and (4.26) and the calculated values are reported in table 4.3.

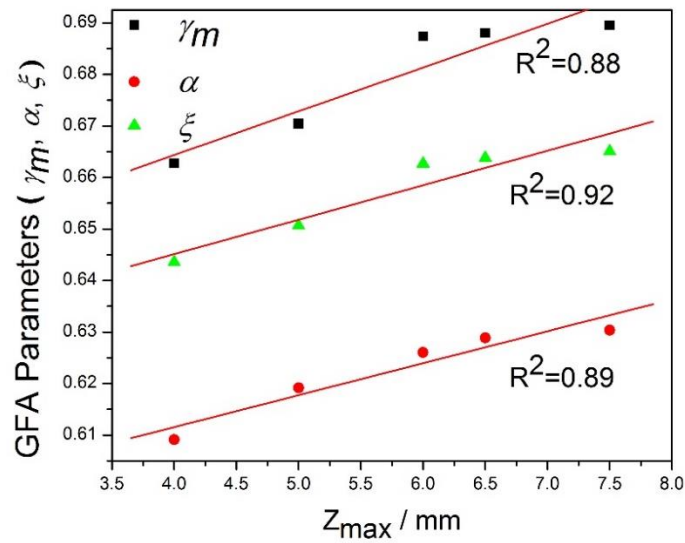
Table 4.3 Gibbs free energy difference at T_g for Zr-based metallic glasses

Alloy Compositions	$\Delta G (T_g)$	$\Delta G (T_g)$
	[Eq (4.25)] (kJmol ⁻¹)	[Eq (4.26)] (kJmol ⁻¹)
Zr _{62.5} Al _{12.1} Cu _{7.95} Ni _{17.45}	5.166	4.359
Zr ₆₃ Al _{11.4} Cu _{9.3} Ni _{16.3}	5.203	4.390
Zr _{63.5} Al _{10.7} Cu _{10.7} Ni _{15.1}	5.252	4.432
Zr ₆₄ Al _{10.1} Cu _{11.7} Ni _{14.2}	5.272	4.449
Zr ₆₅ Al _{8.7} Cu _{14.4} Ni _{11.9}	5.365	4.537

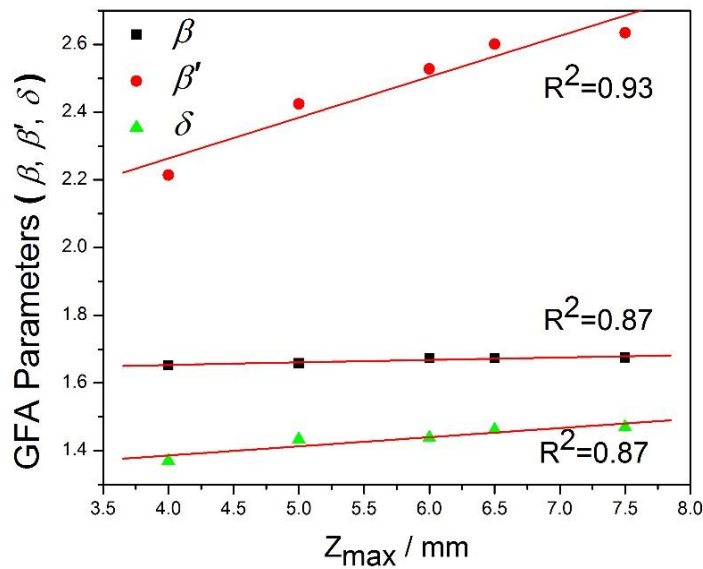
The value of correlation coefficient R^2 is found to be equal to 0.955 and 0.944 as calculated by expressions given by Lad et al (eqs. (4.25) & (4.26) respectively). Among the two expressions of ΔG Lad-1 (eq. (4.25)) is found to have better linear fit with Z_{max} as compared to Lad-2 expression (eq. (4.26)). This indicates that Lad-1 expression provides better one-

to-one correspondence of $\Delta G(T_g)$ values with Z_{max} than Lad-2 expression. Hence for Zr-based metallic glasses Lad-1 expression of $\Delta G(T_g)$ explains the GFA better than Lad-2 expression.

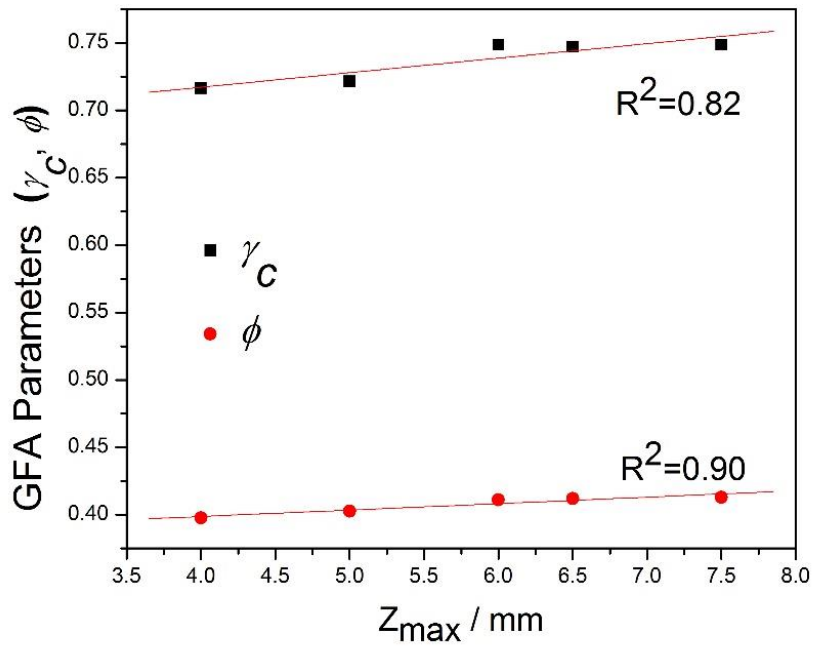
(a)



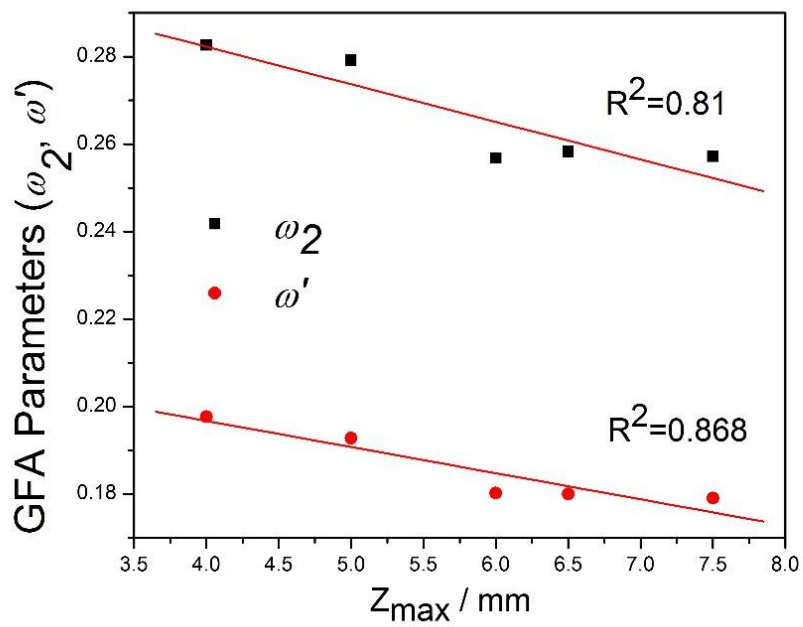
(b)



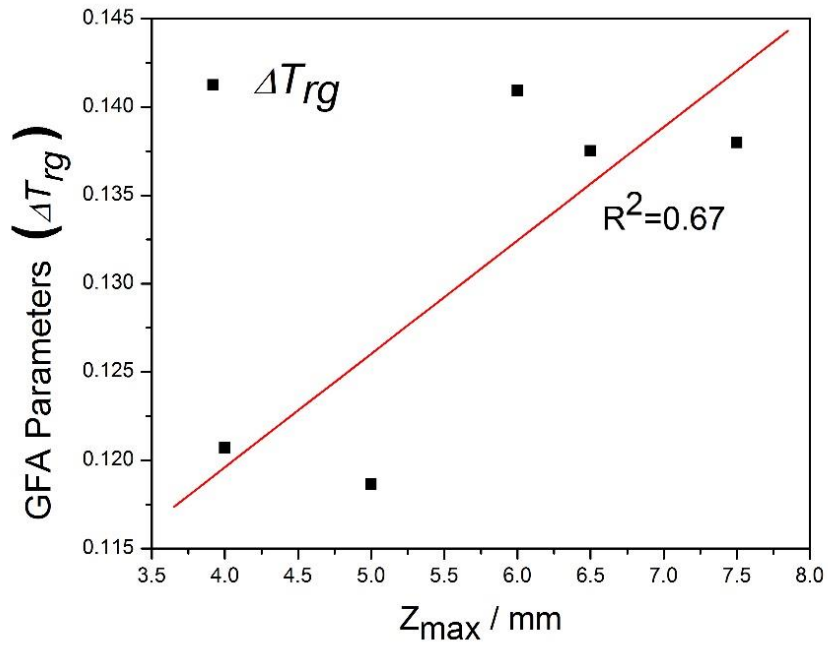
(c)



(d)



(e)



(f)

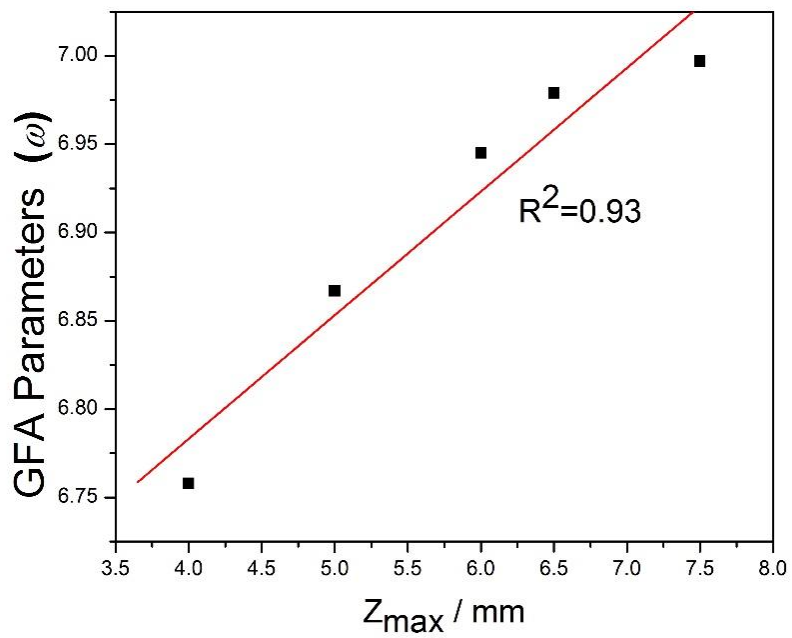


Fig. 4.5: (a) - (f) Relationship between various GFA parameters with Z_{max} for Zr-based metallic glasses

The parameters ω_2 , ω' , and $\Delta G(T_g)$, shows a negative correlation with Z_{max} , whereas all other parameters show a positive correlation with Z_{max} . Among all GFA parameters $\Delta G(T_g)$ is found to have the best correlation with Z_{max} (fig 4.6). Therefore $\Delta G(T_g)$ values can be used as an estimate for GFA of Zr-based metallic glasses. Moreover, Cai et al [4.68] found that ΔH_m can also be considered as a good GFA parameter as it varies linearly with Z_{max} with $R^2 = 0.98$. It implies that along with $\Delta G(T_g)$, ΔH_m can also be used as a decisive criterion for GFA of metallic glasses.

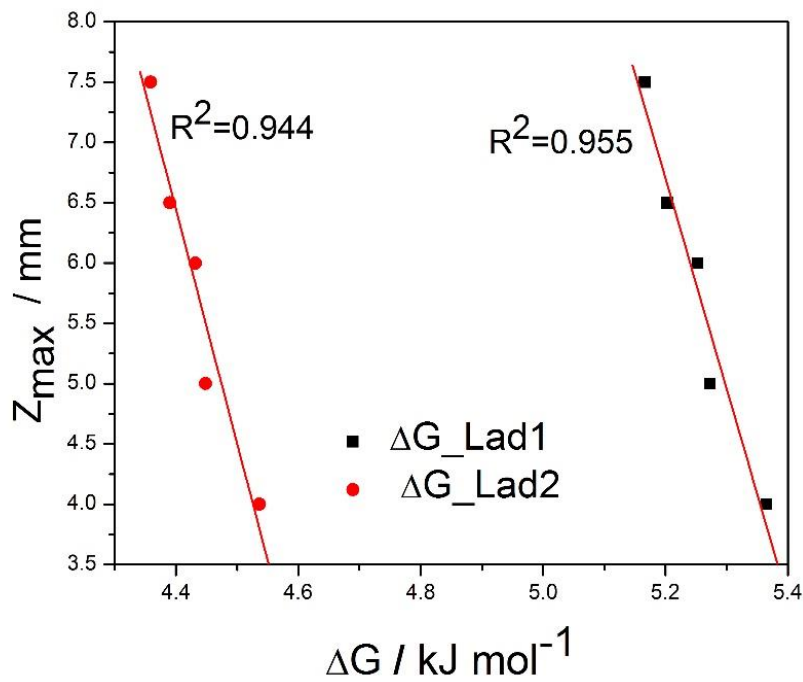


Fig. 4.6: Relationship between $\Delta G(T_g)$ and Z_{max} for Zr-based metallic glasses

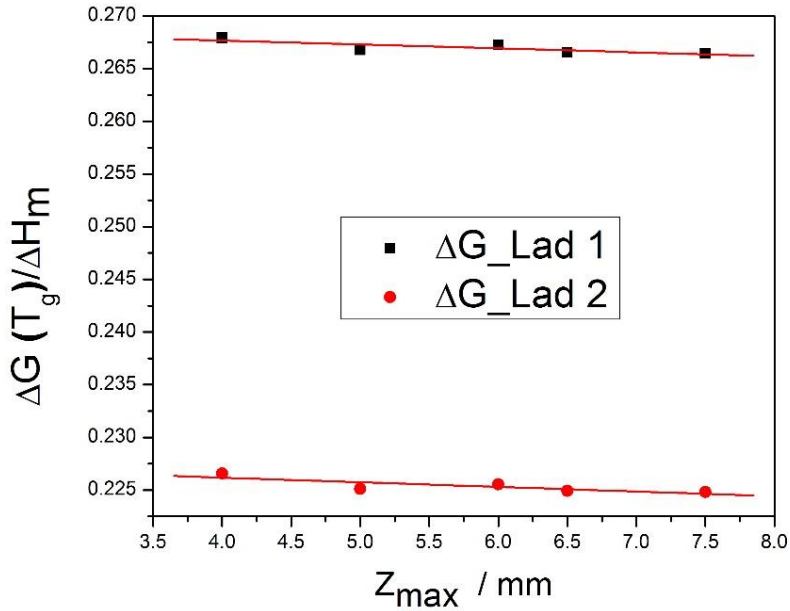


Fig. 4.7: Relationship between $\Delta G (T_g) / \Delta H_m$ and Z_{max} for Zr-based metallic glasses

Further the ratio $\Delta G (T_g) / \Delta H_m$ is found to have a nearly constant value for a single expression of ΔG . Considering equations (4.25) and (4.26), the value of $\Delta G (T_g) / \Delta H_m$ comes out to be 0.27 and 0.22 respectively (fig. 4.7). $Zr_{62.5}Al_{12.1}Cu_{7.95}Ni_{17.45}$ amorphous alloy is found to be the best glass former among the five Zr-based metallic glasses. The composition dependence of GFA of these five BMGs can be observed from the table 4.2. As composition changes, value of the thermodynamic parameter $\Delta G (T_g)$ changes and hence the GFA shows a variation for different metallic glasses. Crystal nucleation requires a large amount of energy. Crystallization of alloy becomes more and more difficult as ΔG decreases, thereby increasing the GFA of metallic alloys. Zr-based metallic glasses can be arranged in order increasing GFA as $Zr_{65}Al_{8.7}Cu_{14.4}Ni_{11.9}$, $Zr_{64}Al_{10.1}Cu_{11.7}Ni_{14.2}$, $Zr_{63.5}Al_{10.7}Cu_{10.7}Ni_{15.1}$, $Zr_{63}Al_{11.4}Cu_{9.3}Ni_{16.3}$, and $Zr_{62.5}Al_{12.1}Cu_{7.95}Ni_{17.45}$.

4.3.3 Effect of Micro-alloying on the GFA of Amorphous

Alloys

As discussed in section 4.12, GFA of amorphous alloys enhance by increasing the number of components. In this section the GFA of Cu-Zr binary alloy and Fe-based multicomponent amorphous alloy has been studied by substituting minor amounts of alloying elements.

4.3.3.1 $(\text{Cu}_{50}\text{Zr}_{50})_{100-x}\text{M}_x$ (where M=Nb and Al, and $x=0, 4$)

The binary alloy $\text{Cu}_{50}\text{Zr}_{50}$ is one of the best glass formers in Cu-Zr systems [4.45]. Furthermore, partial substitution of alloying elements to binary alloys improves their GFA significantly. Yu et al [4.67] showed that minor addition of Al to $\text{Cu}_{50}\text{Zr}_{50}$ BMG enhances its GFA. Further, they procured BMG cylinders having diameter $\geq 5\text{mm}$ by substituting 8 at. % of Al to $\text{Cu}_{50}\text{Zr}_{50}$ BMG. The GFA of $(\text{Cu}_{50}\text{Zr}_{50})_{100-x}\text{M}_x$ metallic glass, where M=Nb and Al, and $x=0, 4$, is studied by using different GFA parameters and the thermodynamic parameter (ΔG). Table 4.4 shows the experimental parameters used for the calculation of various GFA parameters for $(\text{Cu}_{50}\text{Zr}_{50})_{100-x}\text{M}_x$ (where M=Nb and Al, and $x=0, 4$) metallic glasses.

Table 4.4 Characteristic temperatures (K) for $(\text{Cu}_{50}\text{Zr}_{50})_{100-x}\text{M}_x$ metallic glasses, where $\text{M}=\text{Nb}$ and Al , and $x=0, 4$ [4.68]

Alloy compositions	T_g (K)	T_x (K)	T_m (K)	T_l (K)
$\text{Cu}_{50}\text{Zr}_{50}$ (ribbon)	421	471	878	940
$(\text{Cu}_{50}\text{Zr}_{50})_{96}\text{Nb}_4$ (ribbon)	416	466	860	926
$(\text{Cu}_{50}\text{Zr}_{50})_{96}\text{Al}_4$ (ribbon)	425	476	866	915
$(\text{Cu}_{50}\text{Zr}_{50})_{96}\text{Al}_4$ (2mm)	425	473		
$(\text{Cu}_{50}\text{Zr}_{50})_{96}\text{Al}_4$ (4mm)	424	476		
$(\text{Cu}_{50}\text{Zr}_{50})_{96}\text{Al}_4$ (6mm)	424	474		

Table 4.5 report various GFA parameters for $\text{Cu}_{50}\text{Zr}_{50}$, $(\text{Cu}_{50}\text{Zr}_{50})_{96}\text{Nb}_4$, and $(\text{Cu}_{50}\text{Zr}_{50})_{96}\text{Al}_4$ alloys. Low values of η and ω' , ω_2 indicate high GFA. On the contrary, all other parameters like γ_m , α , β , δ , etc., show high values for good glass formers. It is evident from the table 4.5, that Nb and Al addition improves the GFA of $\text{Cu}_{50}\text{Zr}_{50}$ metallic glass. As far as ribbons are concerned almost all parameters give an appropriate variation with GFA. However, most of them are unable to explain the GFA variation of $(\text{Cu}_{50}\text{Zr}_{50})_{96}\text{Al}_4$ alloy as thickness increases, but Q factor $[((T_g+T_x)/T_l) (\Delta H_x/\Delta H_m)]$ and η $[1-(\Delta H_x/\Delta H_m)]$ satisfactorily explain this variation. η is the order parameter that gives information about the orderliness of a metallic glass. Hence lower η values indicate less ordered structure and hence good GFA. Q factor is greatest for $(\text{Cu}_{50}\text{Zr}_{50})_{96}\text{Al}_4$ ribbon and decreases as thickness increases, whereas η is smallest for ribbon and increases with thickness.

Table 4.5 GFA parameters for $(\text{Cu}_{50}\text{Zr}_{50})_{100-x}\text{M}_x$ metallic glasses, where $\text{M}=\text{Nb}$ and Al , and $x=0, 4$

Compositions	γ_m	α	β	β'	Q	η	δ
$\text{Cu}_{50}\text{Zr}_{50}$ (ribbon)	0.65	0.61	1.64	2.35	0.64	0.46	1.43
$(\text{Cu}_{50}\text{Zr}_{50})_{96}\text{Nb}_4$ (ribbon)	0.66	0.62	1.65	2.41	0.68	0.42	1.45
$(\text{Cu}_{50}\text{Zr}_{50})_{96}\text{Al}_4$ (ribbon)	0.67	0.63	1.66	2.71	0.77	0.37	1.53
$(\text{Cu}_{50}\text{Zr}_{50})_{96}\text{Al}_4$ (2mm)	0.67	0.63	1.66	2.67	0.75	0.38	1.52
$(\text{Cu}_{50}\text{Zr}_{50})_{96}\text{Al}_4$ (4mm)	0.67	0.63	1.66	2.71	0.69	0.43	1.53
$(\text{Cu}_{50}\text{Zr}_{50})_{96}\text{Al}_4$ (6mm)	0.67	0.63	1.66	2.68	0.52	0.57	1.52

Table 4.5 continued.....

Compositions	ω	ω'	ω_2	ξ	ϕ	γ_c	ΔT_{rg}
$\text{Cu}_{50}\text{Zr}_{50}$ (ribbon)	6.80	0.20	0.30	0.64	0.39	0.70	0.10
$(\text{Cu}_{50}\text{Zr}_{50})_{96}\text{Nb}_4$ (ribbon)	6.84	0.20	0.30	0.64	0.39	0.70	0.10
$(\text{Cu}_{50}\text{Zr}_{50})_{96}\text{Al}_4$ (ribbon)	7.00	0.19	0.28	0.66	0.40	0.72	0.10
$(\text{Cu}_{50}\text{Zr}_{50})_{96}\text{Al}_4$ (2mm)	6.97	0.20	0.29	0.65	0.40	0.71	0.10
$(\text{Cu}_{50}\text{Zr}_{50})_{96}\text{Al}_4$ (4mm)	7.00	0.19	0.28	0.66	0.40	0.72	0.11
$(\text{Cu}_{50}\text{Zr}_{50})_{96}\text{Al}_4$ (6mm)	6.98	0.19	0.29	0.65	0.40	0.71	0.10

4.3.3.1.1 Gibbs Free Energy Difference (ΔG)

$\Delta G (T_g)$ varies significantly for different compositions as shown in table 4.6. ΔG , which is the driving force of nucleation, is one of the dominating factors that affect kinetics of crystallization. It can be seen that ΔG for $(\text{Cu}_{50}\text{Zr}_{50})_{96}\text{Nb}_4$ is less than that of $\text{Cu}_{50}\text{Zr}_{50}$, and is lowest for $(\text{Cu}_{50}\text{Zr}_{50})_{96}\text{Al}_4$ alloy as calculated by equations (4.25) & (4.26). It indicates that among the three metallic alloys $(\text{Cu}_{50}\text{Zr}_{50})_{96}\text{Al}_4$ is the best glass former.

Table 4.6 Values of $\Delta G (T_g)$ in kJmol^{-1} by Lad-I and lad-II equations

Alloy composition	Lad-I (kJ/mol)	Lad-II (kJ/mol)
Cu₅₀Zr₅₀ (ribbon)	2.00	1.69
(Cu₅₀Zr₅₀)₉₆Nb₄ (ribbon)	1.95	1.64
(Cu₅₀Zr₅₀)₉₆Al₄ (ribbon)	1.68	1.42
(Cu₅₀Zr₅₀)₉₆Al₄ (2mm)	1.68	1.42
(Cu₅₀Zr₅₀)₉₆Al₄ (4mm)	1.68	1.42
(Cu₅₀Zr₅₀)₉₆Al₄ (6mm)	1.68	1.42

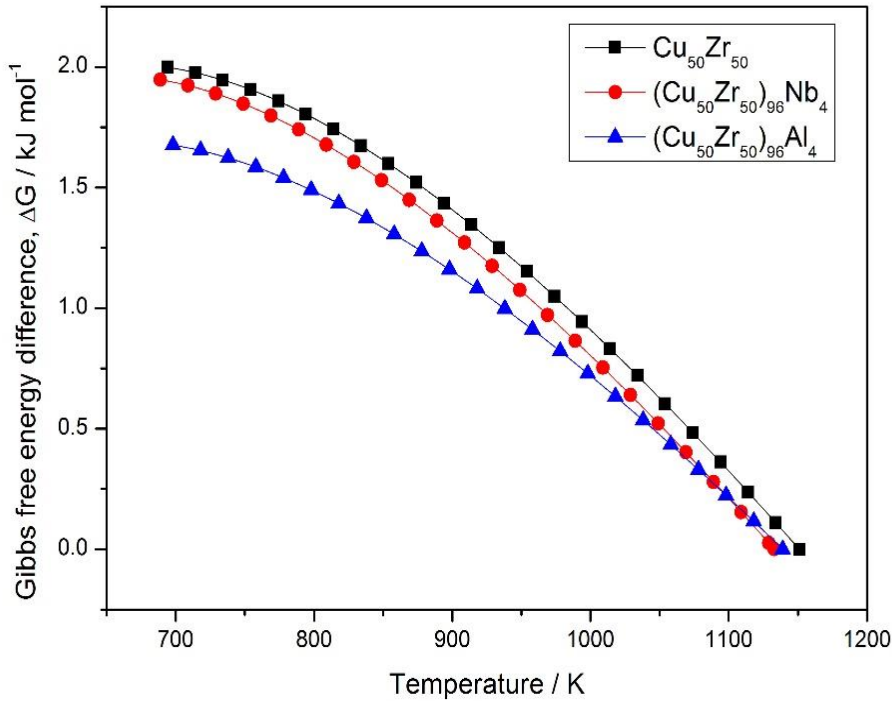


Fig. 4.8: Variation of Gibbs free energy with temperature for $(\text{Cu}_{50}\text{Zr}_{50})_{100-x}\text{M}_x$ metallic glasses, where $\text{M}=\text{Nb}$ and Al , and $x=0, 4$

Fig. 4.8 indicates the variation of ΔG with temperature, for $\text{Cu}_{50}\text{Zr}_{50}$, $(\text{Cu}_{50}\text{Zr}_{50})_{96}\text{Nb}_4$ and $(\text{Cu}_{50}\text{Zr}_{50})_{96}\text{Al}_4$ metallic glasses, in the entire under-cooled region. It is clear from the plot that $(\text{Cu}_{50}\text{Zr}_{50})_{96}\text{Al}_4$ metallic glass has the smallest ΔG values and $\text{Cu}_{50}\text{Zr}_{50}$ metallic glass has the highest ΔG values in comparison with the other respective metallic glasses. Hence among all three metallic glasses, i.e., $\text{Cu}_{50}\text{Zr}_{50}$, $(\text{Cu}_{50}\text{Zr}_{50})_{96}\text{Nb}_4$ and $(\text{Cu}_{50}\text{Zr}_{50})_{96}\text{Al}_4$, $(\text{Cu}_{50}\text{Zr}_{50})_{96}\text{Al}_4$ has the highest GFA.

Further, the variation of ΔG between glass transition temperature (T_g) and melting temperature (T_m) have been shown in fig. 4.9 for $\text{Cu}_{48}\text{Zr}_{48}\text{Al}_4$ alloys. The plot clearly

indicates that the value of ΔG at T_g , obtained by eq. (4.26) is lowest as compared to that obtained by other expressions. Moreover, the nonlinearity in ΔG can be better explained by Eq. (4.25) & (4.26) as the under-cooled region (ΔT) increases.

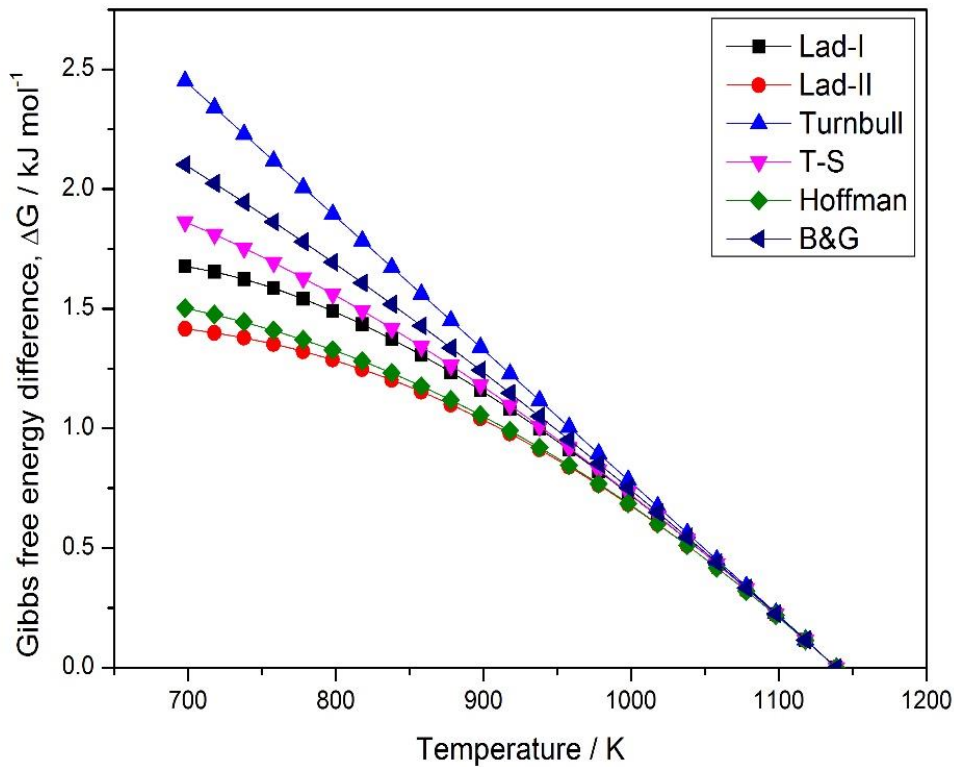


Fig. 4.9: Variation of Gibbs free energy difference with temperature for $\text{Cu}_{48}\text{Zr}_{48}\text{Al}_4$ alloy

4.3.3.2 $\text{Fe}_{48-x}\text{Co}_x\text{Cr}_{15}\text{Mo}_{14}\text{C}_{15}\text{B}_6\text{Y}_2$ ($x=0, 7$) Metallic Glasses

The excellent soft magnetic properties, high electrical resistivity, high strength & hardness, good corrosion resistance and low cost makes Fe-based metallic glasses an appropriate candidate for industrial applications. A large number of Fe-based BMGs have been

developed right from the discovery of first Fe-based BMG by copper mold casting method [4.69]. Ponnambalam et al [4.70] have reported 9 mm thick glassy samples of $\text{Fe}_{48}\text{Cr}_{15}\text{Mo}_{14}\text{C}_{15}\text{B}_6\text{Y}_2$ amorphous alloy. Further, the GFA of this amorphous alloy can be increased by minor substitution of Co for Fe. Shen et al [4.71] have examined the effect on the GFA of $\text{Fe}_{48}\text{Cr}_{15}\text{Mo}_{14}\text{C}_{15}\text{B}_6\text{Y}_2$ amorphous alloy by partial substitution of Co in place of Fe, and reported that the maximum achievable thickness of $\text{Fe}_{48}\text{Cr}_{15}\text{Mo}_{14}\text{C}_{15}\text{B}_6\text{Y}_2$ amorphous alloy can be extended to 16mm on addition of 7 at % of Co in it. The reason for this phenomenal increase in GFA of Fe-based metallic glass has been discussed in light of various GFA parameters and thermodynamic parameter ΔG . The experimental parameters used for the calculation of various GFA parameters for $\text{Fe}_{48-x}\text{Co}_x\text{Cr}_{15}\text{Mo}_{14}\text{C}_{15}\text{B}_6\text{Y}_2$ ($x=0, 7$) metallic glasses are shown in table 4.7.

Table 4.7 Characteristic temperatures (K) for $\text{Fe}_{48-x}\text{Co}_x\text{Cr}_{15}\text{Mo}_{14}\text{C}_{15}\text{B}_6\text{Y}_2$ ($x=0, 7$) [4.71]

Alloy compositions	T_g (K)	T_x (K)	T_m (K)	T_l (K)
$\text{Fe}_{48}\text{Cr}_{15}\text{Mo}_{14}\text{C}_{15}\text{B}_6\text{Y}_2$	839	886	1388	1464
$\text{Fe}_{41}\text{Co}_7\text{Cr}_{15}\text{Mo}_{14}\text{C}_{15}\text{B}_6\text{Y}_2$	838	875	1388	1436

Table 4.8 shows the calculated GFA parameters. As observed from table 4.8 most of the GFA parameters are unable to explain the better glass former among the two alloys. Some of them, such as T_{rg} , β' , δ and ω show a slight variation and show that $\text{Fe}_{41}\text{Co}_7\text{Cr}_{15}\text{Mo}_{14}\text{C}_{15}\text{B}_6\text{Y}_2$ is a better glass former. ΔT_x values represent the thermal stability of metallic alloys. Basically it is the distance between T_g and T_x . The greater the difference

between T_g and T_x , the greater will be the energy required to convert a stable glass into a crystal, and hence higher will be the thermal stability of the glass against crystallization. In present case, $\text{Fe}_{48}\text{Cr}_{15}\text{Mo}_{14}\text{C}_{15}\text{B}_6\text{Y}_2$ is more stable than $\text{Fe}_{41}\text{Co}_7\text{Cr}_{15}\text{Mo}_{14}\text{C}_{15}\text{B}_6\text{Y}_2$. ΔT_x values do not infer GFA of metallic glasses. A good glass former may or may not be thermally stable. Hence, we need to focus on other parameters for determining the GFA of metallic glasses.

Table 4.8 Various GFA parameters for $\text{Fe}_{48-x}\text{Co}_x\text{Cr}_{15}\text{Mo}_{14}\text{C}_{15}\text{B}_6\text{Y}_2$ ($x=0, 7$) metallic glass

Alloy composition	ΔT_x	T_{rg}	γ	α	β	β'	δ	γ_m
$\text{Fe}_{48}\text{Cr}_{15}\text{Mo}_{14}\text{C}_{15}\text{B}_6\text{Y}_2$	47	0.57	0.38	0.61	1.63	2.23	1.42	0.64
$\text{Fe}_{41}\text{Co}_7\text{Cr}_{15}\text{Mo}_{14}\text{C}_{15}\text{B}_6\text{Y}_2$	37	0.58	0.38	0.61	1.63	2.33	1.46	0.64

Table 4.8 continued.....

Alloy composition	ξ	ω'	ω_2	ω	ϕ	γ_c	ΔT_{rg}
$\text{Fe}_{48}\text{Cr}_{15}\text{Mo}_{14}\text{C}_{15}\text{B}_6\text{Y}_2$	0.63	0.22	0.33	6.72	0.38	0.67	0.08
$\text{Fe}_{41}\text{Co}_7\text{Cr}_{15}\text{Mo}_{14}\text{C}_{15}\text{B}_6\text{Y}_2$	0.63	0.22	0.34	6.76	0.37	0.66	0.06

4.3.3.2.1 Gibbs Free Energy Difference (ΔG)

The Gibbs free energy difference (ΔG), between liquid and corresponding crystalline phase, is one of the crucial factors to determine the GFA of metallic glasses. In present case, we have calculated ΔG by expressions given by Lad et al [14-15] and Battezzati & Garonne (B&G) [13]. B & G expression involves the calculation of a parameter γ ($= (1 - (\Delta H_x / \Delta H_m)) / (1 - (T_x / T_m))$), which varies with the experimental parameters ΔH_x , ΔH_m , T_x , and T_m . B & G have assumed this parameter to be constant and equal to 0.8. However, due to its dependence

on ΔH_x , ΔH_m , T_x , and T_m , its value should vary for different metallic glasses and for different crystallization events occurring in a single metallic glass.

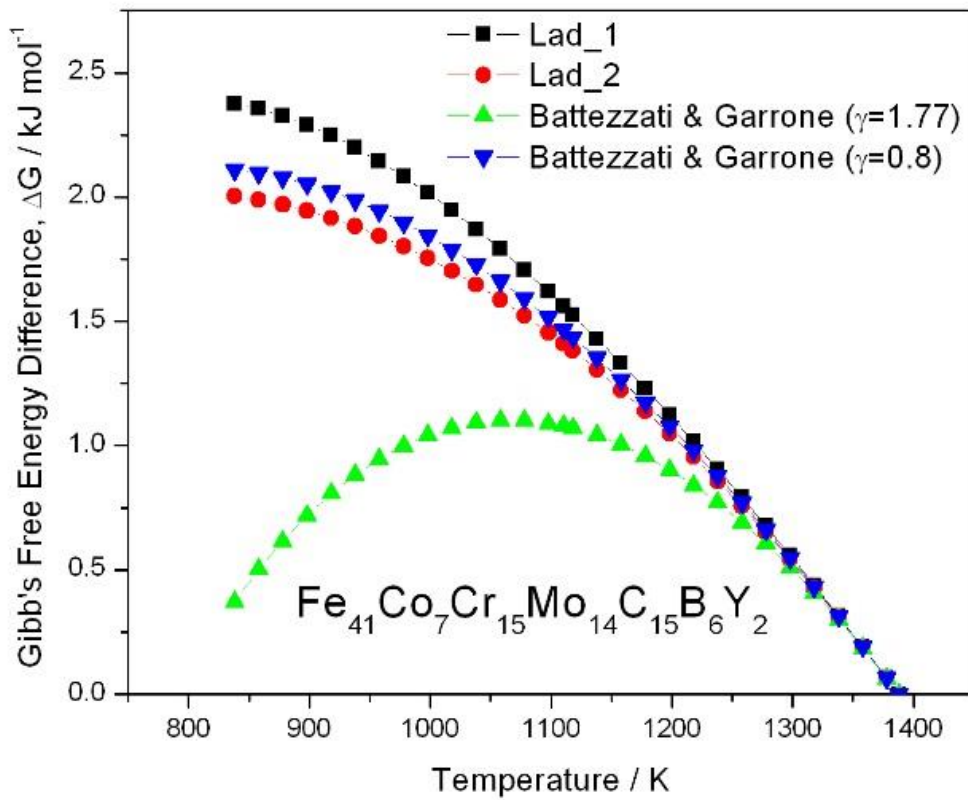


Fig. 4.10: Variation of ΔG with temperature for $\text{Fe}_{41}\text{Co}_7\text{Cr}_{15}\text{Mo}_{14}\text{C}_{15}\text{B}_6\text{Y}_2$ metallic glass

Also, γ must have some dependence on heating rate, since ΔH_x , ΔH_m , T_x , and T_m are heating rate dependent parameters. Hence it cannot be considered to be constant. In present case, the value of γ is coming out to be 1.77 for $\text{Fe}_{41}\text{Co}_7\text{Cr}_{15}\text{Mo}_{14}\text{C}_{15}\text{B}_6\text{Y}_2$.

On using this value of γ for calculation of ΔG in the entire undercooled range, the graph shows a maximum at ~ 1098 K and then decreases with increase in temperature (Fig 4.8). $\Delta G (T_g)$ value comes out to be equal to 0.372 kJmol^{-1} , which is quite low as compared to the values obtained by Lad et al expressions (eqs. (4.25) and (4.26)). Further, when we consider $\gamma=0.8$, the results come in accordance with the other expressions as seen from fig. 4.10. Hence, using B & G expression here is inappropriate here. Therefore we have used expressions given by Lad et al (eqs. (4.25) and (4.26)).

Fig 4.11 shows the variation of $\Delta G (T_g)$ by Lad-1 expression (eq. (4.25)). It can be observed that the ΔG values for $\text{Fe}_{41}\text{Co}_7\text{Cr}_{15}\text{Mo}_{14}\text{C}_{15}\text{B}_6\text{Y}_2$ metallic glass are smaller than that of $\text{Fe}_{48}\text{Cr}_{15}\text{Mo}_{14}\text{C}_{15}\text{B}_6\text{Y}_2$ metallic glass, in the entire undercooled range. This indicates that $\text{Fe}_{41}\text{Co}_7\text{Cr}_{15}\text{Mo}_{14}\text{C}_{15}\text{B}_6\text{Y}_2$ is a better glass former as compared to $\text{Fe}_{48}\text{Cr}_{15}\text{Mo}_{14}\text{C}_{15}\text{B}_6\text{Y}_2$ metallic glass. Table 4.9 reports the values of $\Delta G (T_g)$ calculated by different equations. $\Delta G (T_g)$ values for $\text{Fe}_{48}\text{Cr}_{15}\text{Mo}_{14}\text{C}_{15}\text{B}_6\text{Y}_2$ and $\text{Fe}_{41}\text{Co}_7\text{Cr}_{15}\text{Mo}_{14}\text{C}_{15}\text{B}_6\text{Y}_2$ metallic glass are found to be 2.91 and 2.38 kJmol^{-1} respectively. Other equations also provide smaller $\Delta G (T_g)$ values

for $\text{Fe}_{41}\text{Co}_7\text{Cr}_{15}\text{Mo}_{14}\text{C}_{15}\text{B}_6\text{Y}_2$ metallic glass. This, therefore, implies that minor addition of Co to the Fe-based alloy enhances its glass forming ability significantly.

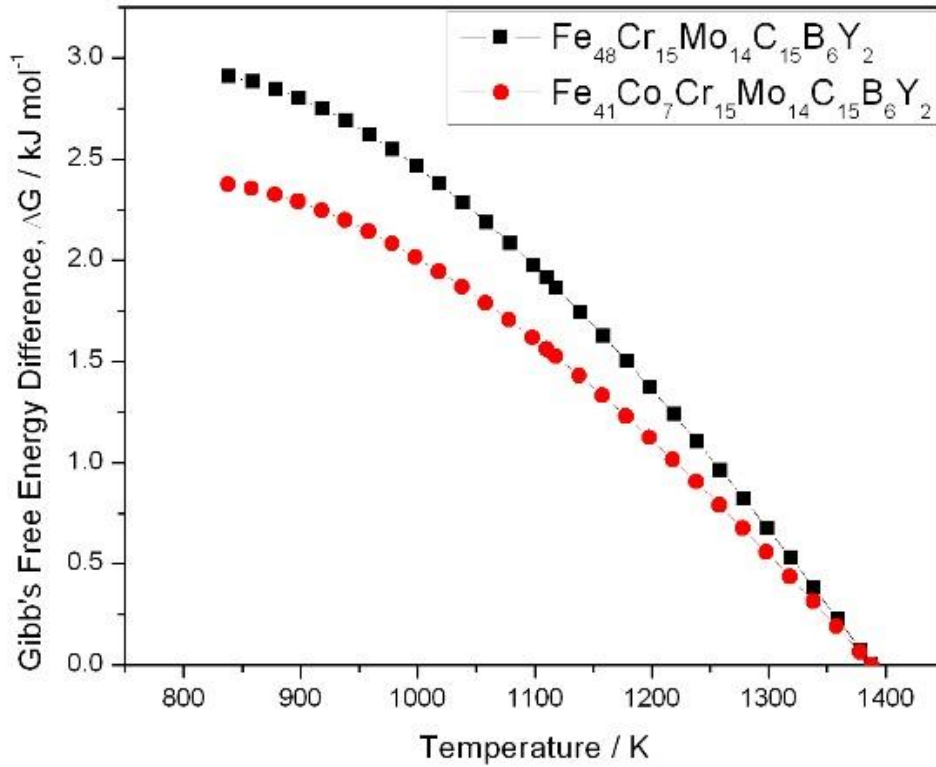


Fig. 4.11: Variation of ΔG (Lad-I) with temperature for $\text{Fe}_{48-x}\text{Co}_x\text{Cr}_{15}\text{Mo}_{14}\text{C}_{15}\text{B}_6\text{Y}_2$ ($x=0, 7$) metallic glass

Table 4.9 $\Delta G(T_g)$ values by different expressions in kJmol^{-1} for $\text{Fe}_{48-x}\text{Co}_x\text{Cr}_{15}\text{Mo}_{14}\text{C}_{15}\text{B}_6\text{Y}_2$ ($x=0, 7$) metallic glass

Alloy composition	Lad-I	Lad-II	B&G ($\gamma=0.8$)
$\text{Fe}_{48}\text{Cr}_{15}\text{Mo}_{14}\text{C}_{15}\text{B}_6\text{Y}_2$	2.91	2.45	2.58
$\text{Fe}_{41}\text{Co}_7\text{Cr}_{15}\text{Mo}_{14}\text{C}_{15}\text{B}_6\text{Y}_2$	2.38	2.00	2.10

4.4 Conclusions

The GFA of metallic glasses has been studied by means of some GFA parameters and thermodynamic parameters. The validity of these parameters can be checked by correlating them with the experimental parameters such as R_c or Z_{max} . Various GFA parameters were correlated with Z_{max} , in order to find their applicability for Zr-based metallic glasses. Statistically, most of them ($\gamma_m, \alpha, \delta, \xi, \Phi, \omega, \omega_2, \omega', \beta, \beta'$) were found to be a good representative of the GFA of metallic glasses. The GFA of metallic glasses is found to be composition and characteristic temperature dependent. $\Delta G (T_g)$ was found to be the best GFA indicator with statistical correlation factor R^2 equal to 0.955 and 0.944 respectively as calculated by Lad-1 (eq. (4.25)) and Lad-2 (eq. (4.26)) expressions. The amorphous alloys with composition $Zr_{62.5}Al_{12.1}Cu_{7.95}Ni_{17.45}$ was the best glass former among all five Zr-based metallic glasses, with $\Delta G (T_g)$ 5.166 and 4.359 kJmol^{-1} respectively by Lad-1 and Lad-2 expression.

The thermodynamic parameter ΔG plays a significant role in predicting the GFA of amorphous alloys. If the variation of ΔC_p with temperature is known, appropriate expression of ΔG can be used for correct determination of GFA of any glass forming system. For $Au_{49}Ag_{5.5}Pd_{2.3}Cu_{26.9}Si_{16.3}$ metallic glass ΔC_p was found to vary hyperbolically with temperature. Hence the expression of ΔG that involves hyperbolic variation of ΔC_p must be used for understanding its GFA. In present case, the thermodynamic behavior of $Au_{49}Ag_{5.5}Pd_{2.3}Cu_{26.9}Si_{16.3}$ metallic glass is studied based on the thermodynamic parameters ΔG , ΔH and ΔS . The results indicate that the expression given by Patel et al, considering hyperbolic

variation of ΔC_p with T matches excellently well in the entire undercooled region, for all three thermodynamic quantities, i. e., ΔG , ΔS and ΔH .

Further, the effect of substitution of minor alloying elements on the GFA of metallic glasses has been studied for Cu-Zr binary metallic glass and Fe-based multicomponent amorphous alloy. Glass forming ability of $\text{Cu}_{50}\text{Zr}_{50}$ was investigated on addition of minor alloying elements Nb and Al. It is observed that 4% of Nb addition enhances the GFA of $\text{Cu}_{50}\text{Zr}_{50}$, which is further improved by 4% of Al addition. ΔG value for $(\text{Cu}_{50}\text{Zr}_{50})_{96}\text{Al}_4$ is lowest that indicate that $(\text{Cu}_{50}\text{Zr}_{50})_{96}\text{Al}_4$ is the best glass former among Cu-Zr amorphous alloys. The driving force of crystallization has been calculated by various methods available in literature. In a similar way, the GFA of Fe-based metallic glass is found to increase by minor addition of Co in it. Most of the GFA parameters were unable to distinguish the better glass former among the two compositions. T_{rg} , β' , δ and ω GFA parameters varied slightly indicating that $\text{Fe}_{41}\text{Co}_7\text{Cr}_{15}\text{Mo}_{14}\text{C}_{15}\text{B}_6\text{Y}_2$ is a better glass former. ΔT_x values indicated that $\text{Fe}_{48}\text{Cr}_{15}\text{Mo}_{14}\text{C}_{15}\text{B}_6\text{Y}_2$ is thermally more stable than $\text{Fe}_{41}\text{Co}_7\text{Cr}_{15}\text{Mo}_{14}\text{C}_{15}\text{B}_6\text{Y}_2$ metallic alloy. On the other hand, $\Delta G(T_g)$ values for $\text{Fe}_{48}\text{Cr}_{15}\text{Mo}_{14}\text{C}_{15}\text{B}_6\text{Y}_2$ metallic glass is found to be higher than that of $\text{Fe}_{41}\text{Co}_7\text{Cr}_{15}\text{Mo}_{14}\text{C}_{15}\text{B}_6\text{Y}_2$ glass, indicating $\text{Fe}_{41}\text{Co}_7\text{Cr}_{15}\text{Mo}_{14}\text{C}_{15}\text{B}_6\text{Y}_2$ is a better glass former. Due to unavailability of experimental ΔG values, the expression involving minimum experimental parameters were used to deduce conclusions regarding the GFA of Cu-Zr binary alloy and Fe-based multicomponent alloy. The expressions given by Lad et al (eqs. (4.25) & (4.26)) were found to be appropriate for describing the variation of ΔG in the undercooled region.

References

- [4.1] C.A. Angell, *J. Non-Cryst. Solids*, **131-133**; 1991: 13.
- [4.2] C.A. Angell, *Science*, **267**; 1995: 1924.
- [4.3] H. Vogel, *Phys. Z.* **22**; 1921: 645.
- [4.4] G. Fulcher, *J. Am. Ceram. Soc.* **8**; 1925: 339.
- [4.5] G. Tammann and W. Z. Hesse, *Anorg. Allg. Chem.* **156**; 1926: 245.
- [4.6] A.K. Doolittle, *J. Appl. Phys.* **22**; 1951: 1471.
- [4.7] K. Russew and F. Sommer, *J. Non-Cryst. Solids*, **319**; 2003: 289.
- [4.8] A. Slipenyuk and J. Eckert, *Scripta Mater.* **50**; 2004: 39.
- [4.9] O. Haruyama and A. Inoue, *Appl. Phys. Lett.* **88**; 2006: 131906.
- [4.10] O. Haruyama, Y. Nakayama, R. Wada, H. Tokunaga, J. Okada, T. Ishikawa and Y. Yokoyama, *Acta Mater.* **58**; 2010: 1829.
- [4.11] A. Masuhr, T.A. Waniuk, R. Busch and W.L. Johnson, *Phys. Rev. Lett.* **82**; 1999: 2290.
- [4.12] Y. Kawamura and A. Inoue, *Appl. Phys. Lett.* **77**; 2000: 1114.
- [4.13] G. Wilde, G.P. G'orler, R. Willnecker and H.J. Fecht, *J. Appl. Phys.* **87**; 2000: 1141.
- [4.14] G.J. Fan and H.J. Fecht, *J. Chem. Phys.* **116**; 2002: 5002.
- [4.15] F. Spaepen, *Scripta Mater.* **54**; 2006: 363.
- [4.16] A. van den Beukel and J. Sietsma, *Acta Metall. Mater.* **38**; 1990: 383.
- [4.17] G. Ruitenberg, P. De Hey, F. Sommer and J. Sietsma, *Phys. Rev. Lett.* **79**; 1997: 4830.
- [4.18] A. van den Beukel, J. Sietsma and P. De Hey, *Acta Metall. Mater.* **46**; 1998: 5873.

- [4.19] P. Wen, W. Wang, Y. Zhao, D. Zhao, M. Pan, F. Li and C. Jin, *Phys. Rev. B*, **69**; 2004: 8.
- [4.20] M. Launey, R. Busch and J. Kruzic, *Scripta Mater.* **54**; 2005: 483.
- [4.21] M. Launey, J. Kruzic, C. Li and R. Busch, *Appl. Phys. Lett.* **91**; 2007: 051913.
- [4.22] M. Launey, R. Busch and J. Kruzic, *Acta Mater.* **56**; 2008: 500.
- [4.23] Y. Zhang and H. Hahn, *J. Non-Cryst. Solids*, **355**; 2009: 2616.
- [4.24] M. C. Weinberg, *Thermochim. Acta*, **280–281**; 1996: 63.
- [4.25] M. C. Weinberg, D. R. Uhlmann and E. D. Zanotto, *J. Am. Ceram. Soc.* **72**; 1989: 2054.
- [4.26] P. I. K. Onorato and D.R. Uhlmann, *J. Non-Cryst. Solids* **22**; 1976: 367.
- [4.27] J. M. Barandiaran and J. Colmenero, *J. Non-Cryst. Solids* **46**; 1981: 277.
- [4.28] X. H. Lin and W.L. Johnson, *J. Appl. Phys.* **78**; 1995: 6514.
- [4.29] W. H. Wang, C. Dong and C. H. Shek, *Mater. Sci. Engg. R*, **44**; 2004: 45.
- [4.30] K. Walter, *Chem. Reviews*, **43 (2)**; 1948: 219.
- [4.31] D. Turnbull, *J. Appl. Phys.* **21**; 1950: 1022.
- [4.32] J. D. Hoffman, *J. Chem. Phys.* **29**; 1958: 1992.
- [4.33] D. R. H. Jones and G. A. Chadwick, *Phil. Mag.* **24**; 1971: 995.
- [4.34] C. V. Thompson and F. Spaepen, *Acta Metall.* **27**; 1979: 1855.
- [4.35] K. N. Lad, A. Pratap and K. G. Raval, *J. Mater. Sci. Lett.* **21**; 2002: 1419.
- [4.36] K. N. Lad, K. G. Raval, A. Pratap, *J. Non-Cryst. Solids*, **334 & 335**; 2004: 259.
- [4.37] L. Battezzati and E. Garrone, *Z. Metallk.* **75**; 1984: 305.

- [4.38] H. Dhurandhar, T. L. Shanker Rao, K. N. Lad and A. Pratap, *Phil. Mag. Lett.* **88** (4); 2008: 239.
- [4.39] H. B. Singh and A. Holz, *Solid State Commun.* **45**; 1983: 985.
- [4.40] X. L. Ji and Y. Pan, *J. Non-Cryst. Solids*, **353**; 2007: 2443.
- [4.41] A. T. Patel, A. Pratap, *AIP Conf. Proc.* **1249**; 2010: 161.
- [4.42] A. Inoue, A. Takeuchi and T. Zhang, *Metall. Mater. Trans.*, **29A**; 1998: 1779.
- [4.43] W. L. Jonson, *MRS Bulletin.* **24** (10); 1999: 42.
- [4.44] L. Xia, S. S. Fang, Q. Wang, Y. D. Dong and C.T. Liu, *Appl. Phys. Lett.* **88** (17); 2006: 171905
- [4.45] A. Inoue, T. Zhang and T. Masumoto, *Mater. Trans. Jpn. Inst. Met.* **31**; 1990: 177.
- [4.46] D. Turnbull, *Contemp. Phys.* **10** (5); 1969: 473.
- [4.47] Z. P. Lu and C. T. Liu, *Acta. Mater.* **50** (13); 2002: 3501.
- [4.48] Z. Z. Yuan, S. L. Bao, Y. Lu, D. P. Zhang and L. Yao, *J. Alloys Compd.* **459**; 2008: 251.
- [4.49] Q. J. Chen, J. Shen, D. Zhang, H. B. Fan, J. F. Sun and D. G. McCartney, *Mater. Sci. Eng. A.* 433; 2006: 155.
- [4.50] X. H. Du, J. C. Huang, C.T. Liu and Z. P. Lu, *J. Appl. Phys.*, **101**; 2007: 086108.
- [4.51] K. Mondal and B. S. Murty, *J. Non-cryst. Solids.* **351**; 2005: 1366.
- [4.52] X. H. Du and J. C. Huang, *Chin. Phys. B.* **17**; 2008: 249.
- [4.53] Z. L. Long, H. Q. Wei, Y. H. Ding, P. Zhang, G. Q. Xie and A. Inoue, *J. Alloys. Compd.* **475**; 2009: 207.

- [4.54] P. Zhang, H. Q. Wei, X. L. Wei, Z. L. Long and X. P. Su, *J. Non-Cryst. Solids*. **355**; 2009: 2183.
- [4.55] G. J. Fan, H. Choo and P. K. Liaw, *J Non-Cryst. Solids*. **353**; 2007: 102.
- [4.56] S. Guo and C. T. Liu, *Intermetallics*, **18 (5)**; 2010: 2065.
- [4.57] X. L. Ji and Y. Pan, *Trans. Nonferrous. Met. Soc. China.*, **19 (5)**; 2009: 1271.
- [4.58] X. Xiao, S. Fang, G. Wang, Q. Hua and Y. Dong, *J. Alloys Compd.* **376**; 2004: 145.
- [4.59] W. Klement, R. H. Willens and P. Duwez, *Nature (London)* **187**; 1960: 869.
- [4.60] H.S. Chen and D. Turnbull, *J. Chem. Phys.* **48**; 1968: 2560.
- [4.61] J. Schroers, B. Lohwongwatana, W.L. Johnson and A. Peker, *Appl. Phys. Lett.* **87**; 2005: 061912.
- [4.62] T. W. Tang, Y. C. Chang, J. C. Huang, Q. Gao, J. S. C. Jang and Chi Y.A. Tsao, *Mat. Chem. Phys.* **116**; 2009: 569.
- [4.63] S. Mechler, E. Yahel, P. S. Pershan, M. Meron and B. Lin, *Appl. Phys. Lett.* **98**; 2011: 251915.
- [4.64] G. D. Fontana, G.L. Fiore and L. Battezzati, *J. Non-Cryst. Solids*, **382**; 2013: 95.
- [4.65] X. H. Lin and W. L. Johnson, *J. Appl. Phys.*, **78**; 1995: 6514.
- [4.66] A. H. Cai, X. Xiong, Y. Liu, W. K. An, J. Y. Tan and Y. Pan, *J. Alloys Compds.* **468**; 2009: 432.
- [4.67] P. Yu, H.Y. Bai, M.B. Tang and W.L. Wang, *J. Non-Cryst. Solids*, **351**; 2005: 1328.
- [4.68] T. A. Baser and M. Baricco, *Rev. Adv. Mater. Sci.* **18**; 2008: 71.
- [4.69] A. Inoue and J. S. Gook, *Mater. Trans. JIM*, **36**; 1995: 1180.

- [4.70] V. Ponnambalam, S. J. Poon, and G. J. Shiflet, *J. Mater. Res.* **19**; 2004: 1320.
- [4.71] J. H. Shen, Q. Chen, J. Sun, H. Fan and G. Wang, *Appl. Phys. Lett.* **86**; 2005: 151907.